Formation mechanisms for gold nanoparticles in a redesigned Ultrasonic Spray Pyrolysis

Article *in* Advanced Powder Technology · December 2016

DOI: 10.1016/j.apt.2016.12.013

CITATIONS
15

READS
352

4 authors:

Peter Majeric
University of Maribor
35 PUBLICATIONS **199** CITATIONS
SEE PROFILE

Darja Feizpour
Institute of Metals and Technology
45 PUBLICATIONS **886** CITATIONS
SEE PROFILE

Bernd Friedrich
RWTH Aachen University
843 PUBLICATIONS **4,682** CITATIONS
SEE PROFILE

Rebeka Rudolf
University of Maribor
137 PUBLICATIONS **875** CITATIONS
SEE PROFILE

Advanced Powder Technology xxx (2017) xxx–xxx

Contents lists available at ScienceDirect

Advanced Powder Technology

journal homepage: www.elsevier.com/locate/apt

Original Research Paper

Formation mechanisms for gold nanoparticles in a redesigned Ultrasonic Spray Pyrolysis

Peter Majerič [a,*], Darja Jenko [b], Bernd Friedrich [c], Rebeka Rudolf [a,d]

[a] University of Maribor, Faculty of Mechanical Engineering, Smetanova ulica 17, 2000 Maribor, Slovenia
[b] Institute of Metals and Technology, IMT, Lepi pot 11, 1000 Ljubljana, Slovenia
[c] IME Institute of Process Metallurgy and Metal Recycling, RWTH Aachen, Intzestraße 3, 52056 Aachen, Germany
[d] Zlatarna Celje d.d., Kersnikova 19, 3000 Celje, Slovenia

ARTICLE INFO

Article history:
Received 26 July 2016
Received in revised form 28 November 2016
Accepted 13 December 2016
Available online xxxx

Keywords:
Ultrasonic Spray Pyrolysis (USP)
Influential synthesis parameters
Formation mechanisms
Gold nanoparticles
Transmission Electron Microscopy (TEM)

ABSTRACT

The aim of this article was an explanation of the gold nanoparticle (AuNP) formation mechanisms which take place in a redesigned Ultrasonic Spray Pyrolysis (USP). Depending on the synthesis parameters of gold concentration in the precursor solution, gas flow and reaction temperature, we have previously obtained a combination of spherical, irregular and cylindrical AuNPs. Two parameters (gold concentration and gas flow) were determined to be the most influential on the shapes and sizes of the produced AuNPs. The effects of these two influential synthesis parameters were evaluated on controlling the formation mechanisms: Gold concentration (2.5 and 0.5 g/l Au) in the precursor solution of $HAuCl_4$ dissolved in water and gas flows of (i) aerosol carrier gas N_2 (1.5, 3.0 and 4.5 l/min) and (ii) reduction gas H_2 (1.0, 1.5 and 2.0 l/min). Depending on the parameter conditions, the AuNPs are formed from a combination of the liquid/solid phase (Droplet-to-Particle mechanism, DTP), the gas phase (Gas-to-Particle mechanism, GTP) and from intermediate secondary droplets, formed from primary droplet explosions. Increasing the gas flow affected the evaporation of the solvent (water) and diffusion of the solute ($[AuCl_4]^-$) in the aerosol droplets, which resulted in the formation of more uniformly shaped AuNPs and with narrower size distributions than before. With favorable parameter conditions increased control over AuNP synthesis with USP has been achieved.

1. Introduction

Spray pyrolysis is a known method for synthesis of fine powders and nanoparticles, capable of synthesizing spherical, hollow, core-shell, porous and other structures, of various materials such as metals and ceramics, with high elemental and phase purity [1–5]. Even though this is a relatively known process of powder production of a wide selection of materials, the specifics for nanoparticle formation are not known for a lot of them.

Gold nanoparticles (AuNPs[1]), along with silver and copper, are the most common nanoparticles used to obtain the surface plasmon effect [6]. The AuNPs' unique properties make them useful in the fields of Biotechnology, Energy, Chemistry and Information Technology [1,7], while the main current markets for AuNPs are in Biomedicine, in tissue or tumor imaging, drug delivery, photothermal therapy and immunochromatographic identification of pathogens in clinical specimens [8,9]. The physical and chemical properties of AuNPs are determined by their size, morphology, surface structure and purity. Although there are several methods for producing AuNPs, controlling their synthesis with a uniform size and morphology still remains a challenge. Several studies have been devoted to accomplish this [6,7,10–13]. Generally, the synthesis of AuNPs involves the Sodium Citrate reduction method, phase transfer method, templating method, seed-mediated method or chemical radiation. Synthesis via aerosol routes like Ultrasonic Spray Pyrolysis (USP[2]) enables production of various nanoscaled materials, including gold. It is relatively simple, flexible and can also be used for film processing. Control of nanoparticle properties can be achieved with careful selection and modification of the USP process parameters [4,5].

With USP, nanoparticles are synthesized from micron-sized droplets of a starting solution. These are created via atomization

* Corresponding author. Fax: +386 2 220 7990.
E-mail addresses: peter.majeric@um.si (P. Majerič), darja.jenko@imt.si (D. Jenko), bfriedrich@ime-aachen.de (B. Friedrich), rebeka.rudolf@um.si (R. Rudolf).

[1] AuNPs – gold nanoparticles.

[2] USP – Ultrasonic Spray Pyrolysis.

http://dx.doi.org/10.1016/j.apt.2016.12.013
0921-8831/

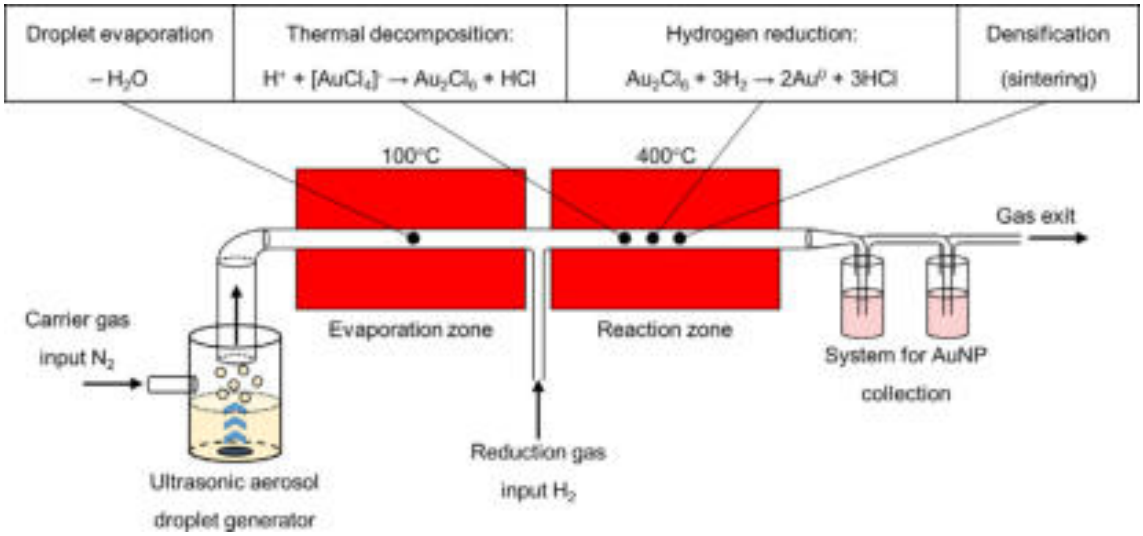

Fig. 1. Modular redesign of USP.

with ultrasound. After the droplets are created they begin to evaporate immediately [14]. After evaporation, a dried nanoparticle is left, which needs to be decomposed or otherwise altered chemically with reduction or oxidation. The final nanoparticle is then formed and collected in a suitable form, as a dried powder, or in a suspension in a suitable medium. These mediums are used to prevent further reactions, such as oxidation, or to stabilize the nanoparticles and prevent agglomeration, where stabilizing agents, such as Sodium Citrate, can be used. The final nanoparticle size is affected heavily by the solids concentration in dilute solutions (1–5 wt.%), but remains roughly unchanged in more concentrated solutions [14]. There are two formation routes which are generally seen in spray pyrolysis: Droplet-to-Particle (DTP[3]) and Gas-to-Particle (GTP[4]) [4,5,15]. In DTP, a single nanoparticle is formed from a single aerosol droplet via evaporation and chemical reactions (decomposition, reduction, or oxidation). In GTP, nanoparticles are formed from the gaseous phase, with formation of new nuclei and several nanoparticles in sizes from a few nm to a few 10 nm are formed from a single aerosol droplet.

As the main synthesis steps in USP are droplet evaporation, precursor conversion and nanoparticle formation, the redesign was done in order to provide more control over the aerosol droplet evaporation and solvent diffusion inside the droplet, for the formation of nanoparticles with a more uniform shape. It is postulated, that the droplet evaporation has the most influence on determining the shape of the final nanoparticles [3,16] and can produce solid, hollow or other shapes of nanoparticles [17]. Several experiments were done in order to determine the AuNP formation mechanisms in the modular redesign of the USP [18,19], Fig. 1.

Previously, we have reported a bimodal size distribution obtained by the redesigned USP system [19]. In order to determine the formation mechanisms, the experiments on the redesigned USP were carried out with changing only the parameters of Au concentration in the precursor and temperature in the evaporation zone. We have ascertained that the bimodal distribution was due to GTP and DTP mechanisms occurring simultaneously in the USP process, when synthesizing AuNPs from $HAuCl_4$. The redesigned USP improved the morphologies of AuNPs compared to the conventional USP, as mainly spherical and some irregular nanoparticle shapes were produced. However, a bimodal size AuNPs' distribution and both formation mechanisms were always present. In order to eliminate bimodal size distribution, the effect of one of these mechanisms needs to be minimized.

In this paper, control of the formation mechanisms of AuNP synthesis with USP was approached by changing the parameters of the precursor Au concentration and gas flows. Based on previous rsearch, it was determined, that the reaction temperature in the range from 300 to 500 °C has a lesser influence on the shapes and sizes of the produced AuNPs in our USP system. It was seen that higher temperatures significantly increase agglomeration. For this reason, the reaction temperature should be kept below 500 °C. The parameter values were selected based on previous experience [19] in order to produce AuNPs of a few 10 nm in size.

2. Materials and methods (experimental)

The synthesis of AuNPs was carried out on the redesigned USP equipment at the IME Institute of Process Metallurgy and Metal Recycling, RWTH Aachen, Germany [18,19], Fig. 1. Precursor solutions of Au were prepared with dissolving hydrogen tetrachloroaurate ($HAuCl_4$, ~50% Au basis, Sigma-Aldrich) in deionized (DI) water. The concentrations of Au in the precursor solutions were 0.5 and 2.5 g/l (0.05 and 0.25 wt.% respectively). The prepared solutions were put into the Ultrasonic Aerosol Generator (Gapusol, RBI France, piezoelectric transducer membrane frequency 2.5 MHz), where they were subjected to an ultrasound to produce aerosol droplets of diameters ranging from 1 to 15 μm, with an average size of 5–6 μm [20]. The aerosol was transported to the heating zones with N_2 gas through quartz glass tubes of 2 cm diameter. Hydrogen gas was added for reduction of gold chloride to pure gold metal nanoparticles. The first heating zone, used for droplet evaporation, was set at a temperature of 100 °C whereas the second heating zone was set at a temperature of 400 °C and was used for reactions required for obtaining pure AuNPs (the length of each heating zone was 28 cm). To determine the gas effects on the synthesized nanoparticles' sizes, three gas flows were used (low: 1.5 l/min N_2 + 1.0 l/min H_2, medium: 3.0 l/min N_2 + 1.5 l/min H_2 and high: 4.5 l/min N_2 + 2.0 l/min H_2). Table 1 shows the experiments performed.

The nanoparticles were collected in 0.1% solution of Na-citrate with DI water for stabilization purposes [21]. No subsequent use and testing of the produced nanoparticles were intended, for instance biocompatibility testing, for which different stabilizing

[3] DTP – Droplet To Particle.
[4] GTP – Gas To Particle.

Please cite this article in press as: P. Majerič et al., Formation mechanisms for gold nanoparticles in a redesigned Ultrasonic Spray Pyrolysis, Advanced Powder Technology (2017), http://dx.doi.org/10.1016/j.apt.2016.12.013

Table 1
List of experiments performed.

Experiment	Ultrasound frequency	Au concentration in precursor solution	Nitrogen N_2 gas flow	Hydrogen H_2 gas flow	First furnace temperature	Second furnace temperature
Low gas flow, low Au concentration	2.5 MHz	0.5 g/l Au	Low: 1.5 l/min	Low: 1.0 l/min	100 °C	400 °C
Low gas flow, high Au concentration		2.5 g/l Au	Low: 1.5 l/min	Low: 1.0 l/min		
Medium gas flow, low Au concentration		0.5 g/l Au	Medium: 3.0 l/min	Medium: 1.5 l/min		
Medium gas flow, high Au concentration		2.5 g/l Au	Medium: 3.0 l/min	Medium: 1.5 l/min		
High gas flow, low Au concentration		0.5 g/l Au	High: 4.5 l/min	High: 2.0 l/min		
High gas flow, high Au concentration		2.5 g/l Au	High: 4.5 l/min	High: 2.0 l/min		

agents would have been selected, such as bi-functional polyethylene glycols (PEGs – with a thiol group and amine, carboxylic, etc. group at each end of the polymer [22]).

2.1. TGA of $HAuCl_4$

Thermogravimetric analyze (TGA) of $HAuCl_4$ was performed with inert gas N_2 at a heating rate of 10 °C/min, from 40 to 600 °C. The parameters were chosen so as to simulate the conditions in the redesigned USP equipment. The thermal decomposition and mass loss are presented in Fig. 2.

2.2. TEM/HRTEM characterization

Conventional Transmission Electron Microscopy (CTEM; JEOL 2100), High-Resolution Transmission Electron Microscopy (HRTEM; JEOL 2100), Electron Diffraction (ED/TEM; JEOL 2100) and Energy Dispersive Spectroscopy (EDS/TEM; JED-2300) investigations were conducted on the prepared AuNPs. A drop of colloidal suspension of AuNPs (in 0.1% solution of Na-citrate with DI water) was pipetted onto a formvar film coated with a layer of carbon or a lacey formvar film enforced by a heavy coating of carbon TEM copper grid of 200 mesh and dried at room temperature. The grid was then observed directly in a TEM once the medium had evaporated.

2.3. Size measurements

The AuNPs' size distributions were measured from 10 to 15 TEM micrographs of each sample. Measurement of sizes and shape determination was done with ImageJ software [23]. The roundness number is calculated from a best fitting ellipse, where 1.0 is equal to a perfect circle, while numbers closer to 0.0 indicate an increasingly elongated shape. The number of nanoparticles for size measurements ranged from 300 to 600 nanoparticles for each particle size distribution. A few TEM micrographs were selected for sample representation purposes. Measurements were performed following measurement protocols in [24].

2.4. DLS size and zeta potential measurements

DLS size measurements were done with Malvern ZetaSizer Nano ZS, for comparison with manually measured sizes from TEM micrographs. Samples were prepared by pipetting 1 ml of AuNP suspensions into disposable sizing cuvettes. A check for any air bubbles in the cuvette was performed before measuring was carried out.

3. Results and discussion

Fig. 2 shows the mass loss of $HAuCl_4$ with TGA. It is seen that the first thermal decomposition begins at 79.88 °C, with a peak

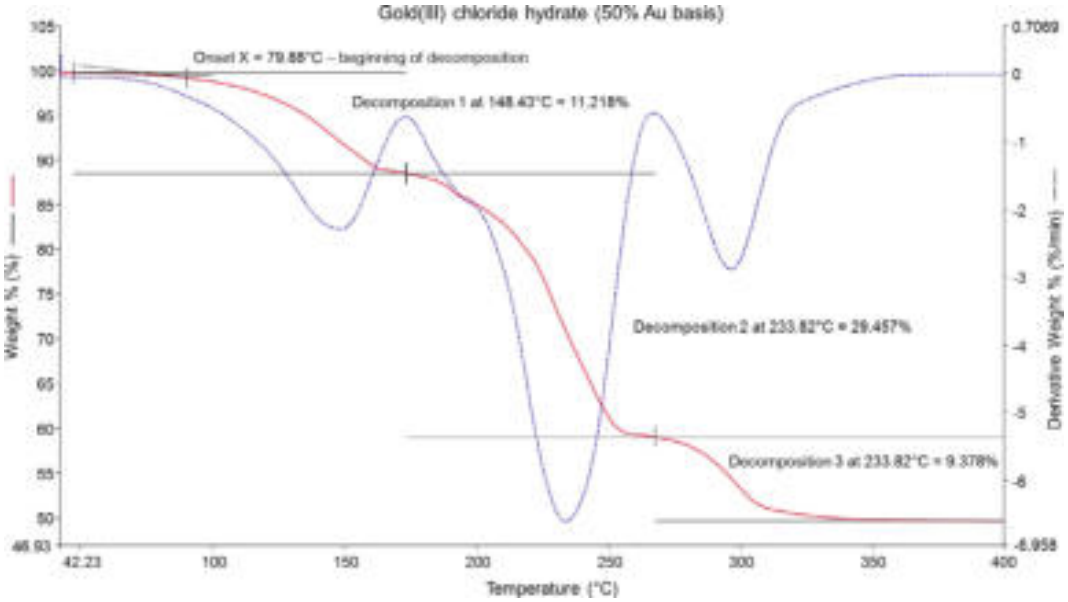

Fig. 2. TGA analysis of $HAuCl_4$, heating rate of 10 °C/min.

Please cite this article in press as: P. Majerič et al., Formation mechanisms for gold nanoparticles in a redesigned Ultrasonic Spray Pyrolysis, Advanced Powder Technology (2017), http://dx.doi.org/10.1016/j.apt.2016.12.013

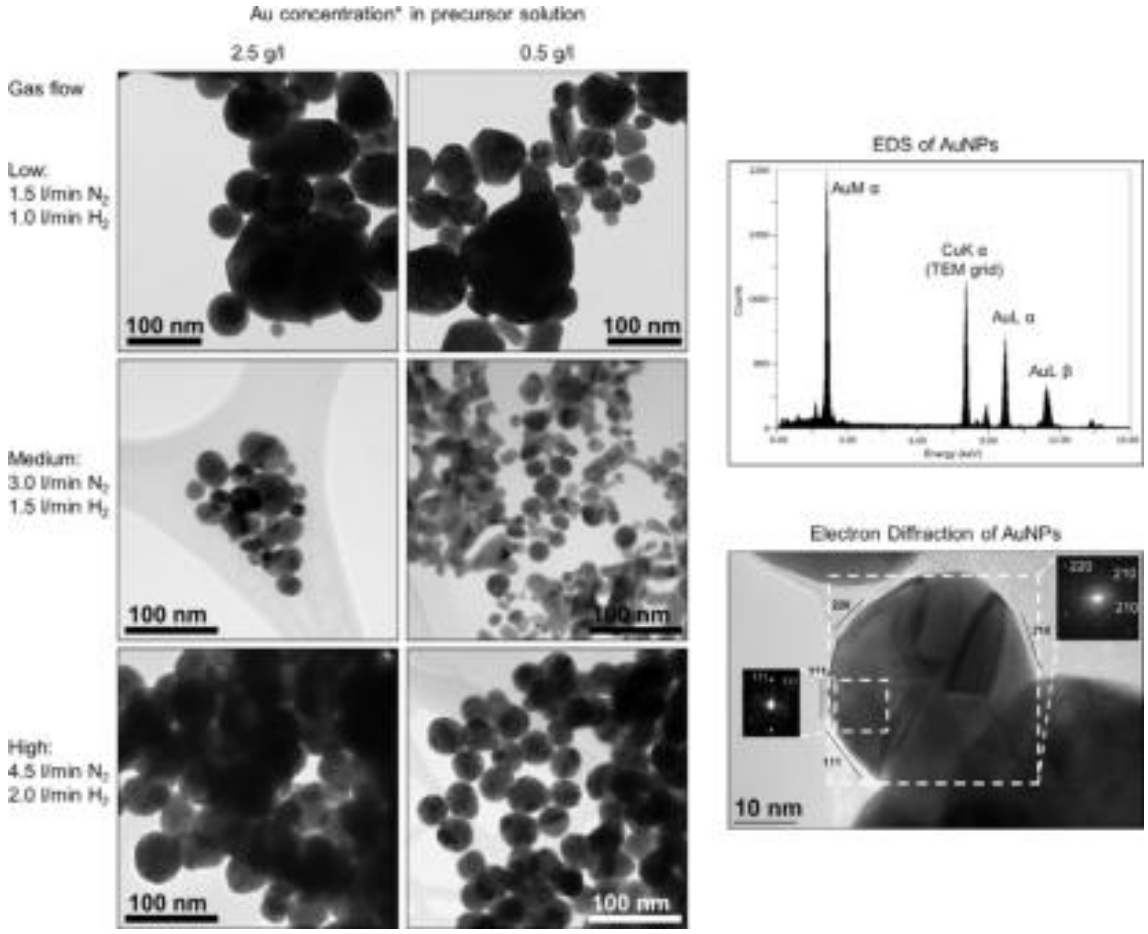

Fig. 3. Representative TEM/HRTEM micrographs with typical EDS analyze and electron diffraction of obtained AuNPs with varied gas flows and concentrations by the redesigned USP, *Au in the precursor solution is in the form of gold chloride, $[AuCl_4]^-$.

decomposition temperature of 148.43 °C. The mass loss is 11.218%, which can be attributed to dechlorination and formation of gold (III) chloride $AuCl_3$ ($HAuCl_4 \rightarrow HCl + AuCl_3$) (theoretical mass loss of 10.7%). The second decomposition peak temperature of 233.82 °C yields a mass loss of 29.46%, which corresponds to the formation of AuCl (theoretically the mass loss is 23.4%). The third decomposition at a peak temperature of 296.56 °C yields Au (49.95% of $HAuCl_4$, theoretically 57.97% of $HAuCl_4$ is Au). These results suggest that thermal composition may begin in the evaporation zone of the USP during aerosol droplet shrinking and drying, while the formation of pure gold is not possible. The gas flow and fast heating rates in USP mean that the first decomposition starts at somewhat higher temperatures than those measured by TGA and is carried out at a faster rate. Even though TGA shows that $HAuCl_4$ decomposes into pure Au, the reaction times in USP are very short, and a reduction gas H_2 is needed for obtaining pure AuNPs. This was also confirmed experimentally, where no AuNPs were formed without the use of H_2 gas.

Fig. 3 shows TEM/HRTEM micrographs with visible sizes and morphology of the obtained AuNPs. EDS analyzes of the nanoparticles show a high purity content of 99.99 wt.% Au. High Au concentration in the precursor solution produced nanoparticles of larger sizes than low Au concentration, as was expected. It is seen, that higher gas flows produce more uniform, spherical shapes of nanoparticles (for 0.5 g/l Au, roundness is 0.924 with a minimum value of 0.694, Table 2), while there are more irregular shapes present when using lower gas flows (for 0.5 g/l Au, roundness is 0.833 with a minimum value of 0.394, Table 2). The expected theoretical sizes for 2.5 and 0.5 g/l Au in the precursor solution are 210 nm and 123 nm for a mean aerosol droplet size of 5 μm. The obtained sizes are much smaller than the calculated ones, so the theoretical approach was not pursued further. Size distributions have been quoted as the mean nanoparticle diameter ± the Standard Deviation (SD), as shown in Table 2. Two means are quoted in samples where two distributions were found. Although bimodal size distributions of the AuNPs were still present, especially with using low gas flows, the number of larger nanoparticles was decreased dramatically with the use of higher gas flows in the USP system.

3.1. Low gas flow

With the precursor solution concentration of 2.5 g/l Au, the obtained nanoparticles had a bimodal size distribution with smaller nanoparticles (a mean size of 39.4 nm, 66.0% of total AuNPs and larger particles (a mean size of 207.9 nm, 34.0% of AuNPs) (Table 2, Fig. 4). When using a concentration of 0.5 g/l Au, the bimodal distribution is not as apparent. However, in the distribution, two peaks are visible (Fig. 4), indicating two size ranges (a mean size of 38.9 nm for GTP, 63.3% of AuNPs and a mean size of 91.3 nm for DTP, 36.7%, Table 2). As such, we can identify a bimodal size distribution present in the USP synthesis of AuNPs when using low gas flows (Reynolds number in evaporation zone, Re = 87.5).

3.2. Medium gas flow

When using medium gas flows (Re = 174.9) the obtained nanoparticles had a mean size of 26.7 nm for 2.5 g/l Au and 17.7 nm for 0.5 g/l Au in the precursor solution. Larger particles

Please cite this article in press as: P. Majerič et al., Formation mechanisms for gold nanoparticles in a redesigned Ultrasonic Spray Pyrolysis, Advanced Powder Technology (2017), http://dx.doi.org/10.1016/j.apt.2016.12.013

Table 2
Aerosol residence time, mean AuNP sizes with SD calculated from measured sizes (with bimodal size distribution, where apparent) and roundness, obtained with TEM images.

Gas flow	Aerosol residence time	AuNP mean sizes ± SD, at 2.5 g/l Au[a]	AuNP mean sizes ± SD, at 0.5 g/l Au[a]	AuNP roundness ± SD, at 2.5 g/l Au[a]	AuNP roundness ± SD, at 0.5 g/l Au[a]
Low: 1.5 l/min N_2 + 1.0 l/min H_2	Evaporation: 3.52 s	39.4 ± 20.6 nm 207.9 ± 38.3 nm	38.9 ± 15.1 nm 91.3 ± 15.2 nm	0.846 ± 0.103	0.833 ± 0.132
	Reaction: 2.11 s	min: 10 nm	min: 14 nm	min: 0.425	min: 0.394
	Total: 5.62 s	max: 293 nm	max: 168 nm	max: 0.991	max: 0.986
Medium: 3.0 l/min N_2 + 1.5 l/min H_2	Evaporation: 1.76 s	26.7 ± 13.1 nm	17.7 ± 6.9 nm	0.879 ± 0.089	0.853 ± 0.104
	Reaction: 1.17 s	min: 8 nm	min: 4 nm	min: 0.611	min: 0.547
	Total: 2.93 s	max: 68 nm	max: 34 nm	max: 0.990	max: 0.988
High: 4.5 l/min N_2 + 2.0 l/min H_2	Evaporation: 1.17 s	45.5 ± 12.5 nm	37.0 ± 5.5 nm	0.889 ± 0.069	0.924 ± 0.053
	Reaction: 0.81 s	min: 15 nm	min: 18 nm	min: 0.674	min: 0.694
	Total: 1.98 s	max: 93 nm	max: 67 nm	max: 0.995	max: 0.998

[a] Au concentration in precursor solution.

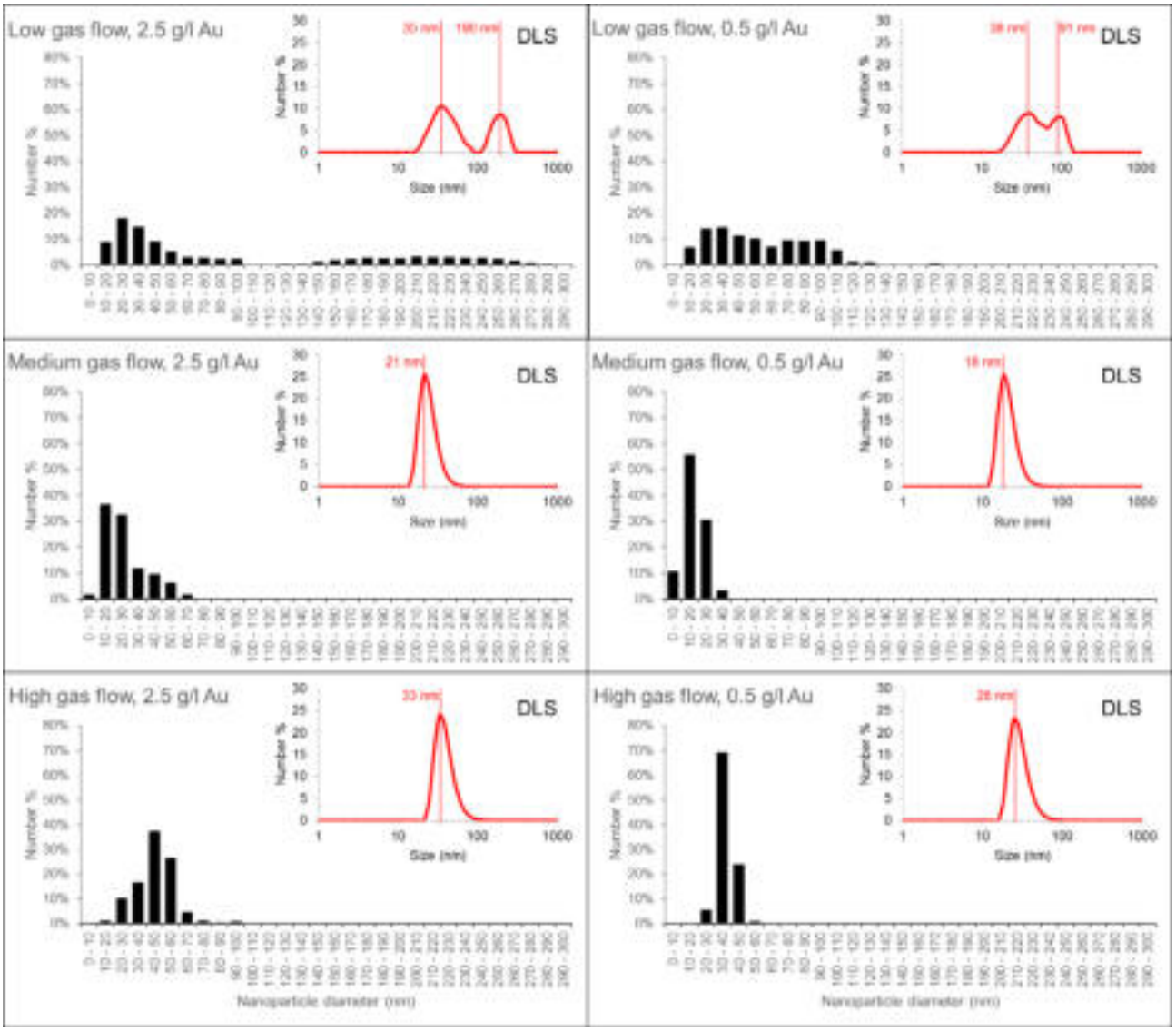

Fig. 4. Size distributions of AuNPs measured from TEM micrographs with accompanying DLS size measurements for comparison, accuracy of measured AuNP sizes from TEM images is estimated at ±2 nm.

Please cite this article in press as: P. Majerič et al., Formation mechanisms for gold nanoparticles in a redesigned Ultrasonic Spray Pyrolysis, Advanced Powder Technology (2017), http://dx.doi.org/10.1016/j.apt.2016.12.013

were characterized as agglomerates of these nanoparticles. There was no apparent bimodal size distribution. For higher Au concentrations in the precursor solution, bigger nanoparticles were obtained than for lower concentrations, which was to be expected, according to literature and previous results. A large number of nanoparticles were in the narrow size range from 10 to 30 nm (69.0%) for 2.5 g/l Au and in the size range from 10 to 20 nm (55.6%) for 0.5 g/l Au in the precursor solution.

3.3. High gas flow

With higher gas flows (Re = 262.4) the nanoparticle sizes were increased somewhat in comparison to medium gas flows, with a mean size of 45.5 nm for 2.5 g/l Au and 37.0 nm for 0.5 g/l Au in the precursor solution. When using higher gas flows there is more turbulence in the USP system compared with medium gas flow, causing more collisions of aerosol droplets, precursor vapors and nanoparticles. The increased number of eddies in the gas flow, especially due to the inlet of the reduction gas H_2 between the furnaces, may also be the cause of the increase of nanoparticle sizes. High gas flow thus causes the formation of larger nanoparticles than medium gas flow, as is visible when comparing the histograms from medium and high gas flows in Fig. 4. A large number of nanoparticles were in the narrow size range from 40 to 60 nm (64.2%) for 2.5 g/l Au and in the size range from 30 to 40 nm (69.1%) for 0.5 g/l Au in the precursor solution.

3.4. Formation mechanisms

Medium and high gas flows provided a narrower AuNP size distribution compared to a low gas flow, as is apparent from the lower SDs in Table 2 and narrower size distributions from the histograms in Fig. 4. The bimodal distribution of nanoparticles is also not as apparent with medium and high gas flows, while the nanoparticle diameters are only a few 10 nm in size.

Previously, we have assumed the bimodal distribution to be a result of two formation mechanisms taking place in the USP – the DTP and GTP mechanisms, which are based on the formation of precursor vapors. The TGA shows decomposition of $HAuCl_4$, with the release of HCl and Cl_2, without a gas phase change at temperatures below 400 °C. However, gold (III) chloride was reported to sublimate when subjected to temperatures slightly above 100 °C for an extended period of time. When subjected to 280 °C, sublimation is more rapid [25]. Palgrave and Parkin [26] used $HAuCl_4$ for aerosol assisted CVD and reported a gas phase of the gold chloride being present at temperatures from 400 to 600 °C. They also concluded that $HAuCl_4$ has excellent CVD precursor characteristics, apart from its low volatility. As such, the formation of precursor vapors in USP was not excluded due to the very small particle sizes with high curvatures (and high vapor pressures) and known gas phase changes of gold chloride even at temperatures of 100 °C.

New results without bimodal size distributions may indicate other processes taking place in the USP. The very small nanoparticles (Table 2) can still be attributed to the GTP mechanism, while the nanoparticles in sizes around 50 nm can be the result of the DTP of secondary aerosol droplets, formed after the initial droplets explode into smaller ones. As the larger aerosol droplets are not evaporated fully in the evaporation zone, they then heat up rapidly in the reaction zone and burst into smaller secondary droplets from which new, small nanoparticles are formed (Fig. 5).

The vapors ejected from the droplet then form new nuclei, which grow into nanoparticles up to a few 10 nm in diameter. Depending on the gas flow stability, more or less uniform nanoparticles are formed from the vapors (Fig. 6). The Au concentration in the precursor determines the sizes of the final AuNPs. When using 2.5 g/l Au, larger nanoparticles were present in the system than with 0.5 g/l Au. Using high gas flows yielded larger nanoparticles than with medium gas flows. This may indicate that, with medium gas flow, the conditions were most optimal for bursting of the initial droplets into very fine secondary droplets. With high gas flows, the primary droplets did not shrink as much as with medium gas flows during evaporation. After bursting of the primary droplets, this caused the secondary droplets to also be larger, as compared to medium gas flows. Following the DTP mechanism, larger secondary droplets then also produced somewhat larger nanoparticles with high gas flows (Fig. 4 and Table 2).

However, by using a conventional USP, the formation of small, fairly uniform AuNPs was not reported [27]. In those experiments, AuNPs smaller than 40 nm were not formed.

The DTP mechanism produces nanoparticles via droplet formation, transport of these droplets into a heating zone, evaporation of the solvent and thermal conversion and reactions of the solute into final nanoparticles. As the droplet with dissolved gold chloride (solute) is being evaporated, it shrinks and, simultaneously, increases the concentration of gold chloride inside the droplet. The solute can begin to precipitate before uniform saturation is reached across the droplet and, thus, the rates of evaporation and nucleation determine nanoparticle morphology.

With GTP formation, a supersaturation of a gaseous species of the solute causes nucleation and new nanoparticle formation. The nanoparticles are formed in two modes. With nucleation-condensation [5], a dimer of $AuCl_3$ or, alternatively, Au_2Cl_6 [25] is formed into a nuclei, which then grows by condensation of other dimers. With nucleation-coagulation, the nanoparticles are formed and are grown through collisions and coalescence (sintering) in order to become spherical. In our system, we have mainly growth by condensation, with some degree of agglomeration present in the form of soft agglomerates. The AuNPs' structure was also examined with HRTEM and electron diffraction (Fig. 3), which has shown the grain boundaries and twins, with possible growth directions of the formed AuNPs.

In the redesigned USP system with the precursor $HAuCl_4$, a combination of both DTP and GTP are present. The ratio of DTP and GTP mechanisms depends on the evaporation (controlled by parameters: Gold chloride concentration in the starting solution, evaporation temperature, gas flow) of the aerosol droplet and gold

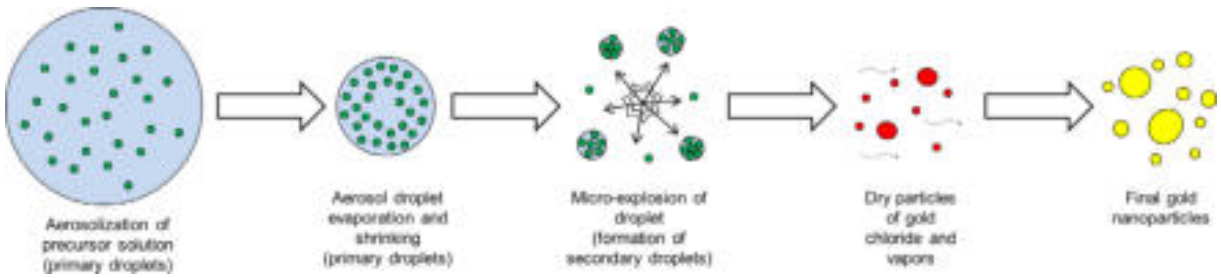

Fig. 5. Schematic illustration of an aerosol droplet bursting into secondary droplets, and the formation of AuNPs.

Please cite this article in press as: P. Majerič et al., Formation mechanisms for gold nanoparticles in a redesigned Ultrasonic Spray Pyrolysis, Advanced Powder Technology (2017), http://dx.doi.org/10.1016/j.apt.2016.12.013

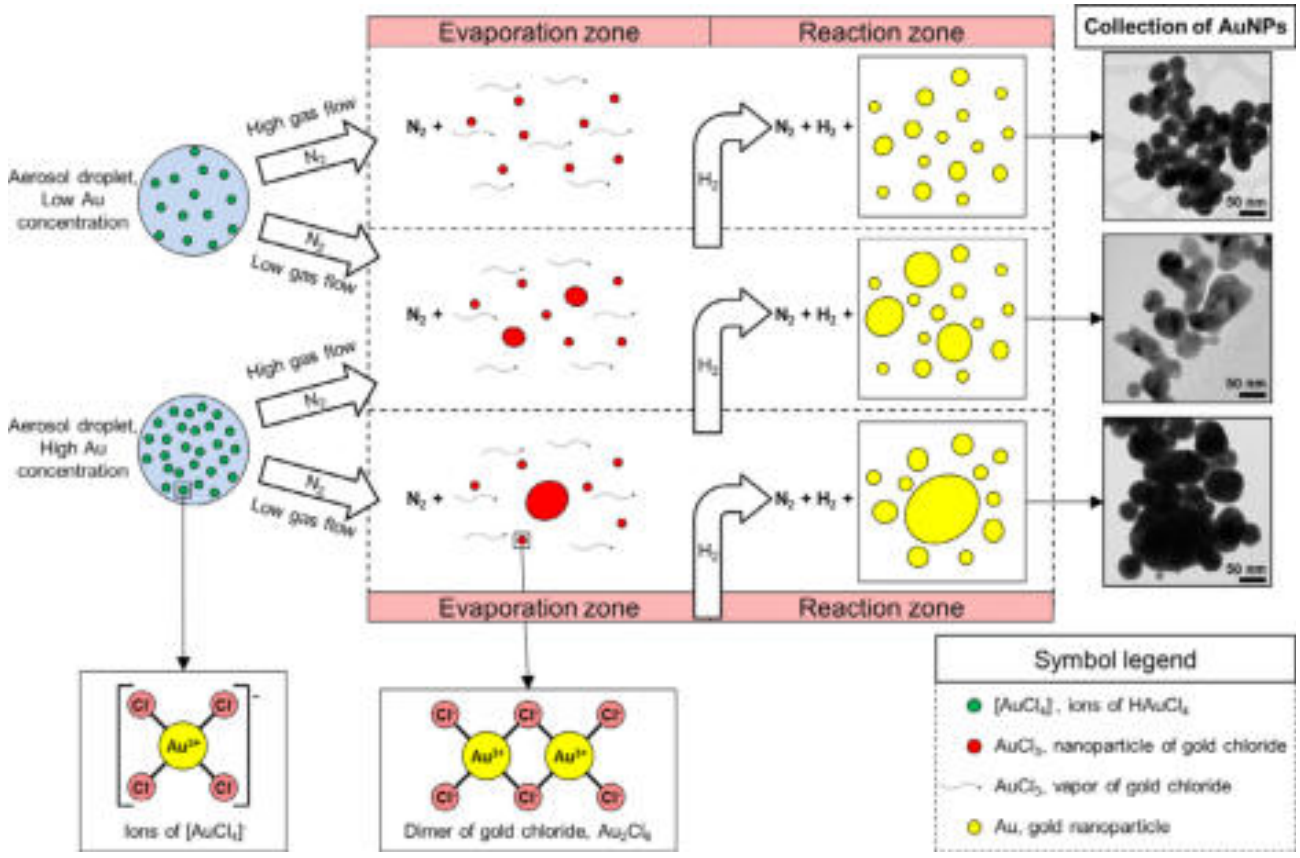

Fig. 6. Schematic illustration of proposed AuNP formation mechanisms, depending on different Au concentrations and gas flows.

chloride inside the droplet and the bursting of initial droplets into secondary droplets. Due to solute vaporization, a mass flow and partial vapor pressure of the gaseous gold chloride is also present in the USP system.

In our previous experiments with the redesigned USP, different parameters were used in order to manipulate the evaporation process. While the evaporation rate, solute diffusion, supersaturation and vaporization are important factors for particle morphology, other phenomena need to be considered. When manipulating the rate of evaporation via changing the temperature (higher temperatures – faster evaporation and vice versa) with a low, steady gas flow used in the experiments, a higher influence of the DTP mechanism is apparent on the nanoparticle formation [19]. Manipulating the evaporation rate via gas flow achieves different results. It seems that by using high gas flows, the evaporation of droplets, their bursting and vaporization of the solvent from the droplet is more dispersed in the system, yielding more uniformly sized, smaller nanoparticles.

A faster evaporation rate induced by a high gas flow favors the GTP mechanism (rapid evaporation and flow conditions promote precursor vaporization) and droplet bursting, while a slower evaporation rate by using low gas flows and low temperatures favors the DTP mechanism (diffusion of precursor into the droplet center and creation of the dried particle). It is important to note that the ratio of the DTP and GTP mechanisms is difficult to determine from the final nanoparticles, as the smaller AuNPs can also be formed by the DTP mechanism, although their growth rate is slower. The nanoparticles formed by GTP catch up to the nanoparticles formed by DTP, due to their higher growth rate. Because of their similar sizes it is then difficult to distinguish which AuNPs have been formed by which mechanism. In theory, GTP produces smaller sizes, matching our results; however, DTP cannot be excluded entirely.

It is visually apparent in the TEM images that a much greater number of spherical shapes is present when increasing gas flow (only a few images have been included in this paper for representation purposes), while also the calculated roundness number has increased when increasing gas flow (Table 2). For a precursor concentration of 2.5 g/l Au, the mean roundness number has increased from 0.846 to 0.879 and 0.889 with increasing the gas flows. More importantly, the minimum roundness value has increased (0.425–0.611–0.674), indicating that even the most irregular shapes of the nanoparticles were more spherical with high gas flows, than with low gas flows. This is also apparent for 0.5 g/l Au, where the mean values increased from 0.833 to 0.853 to 0.924 with increasing gas flow (minimum values: 0.394–0.547–0.694). More work is needed to achieve ideally spherical shapes with a roundness number of 1.0; however, this signifies good progress in the right direction.

For further studies, AuNP formation mechanisms will be examined using precursors other than $HAuCl_4$. Additional stabilization agents will also be used for synthesis of AuNPs in the range of 10–50 nm, intended for biocompatibility testing and potential use in biomedical applications.

4. Conclusions

AuNPs were synthesized by varying the precursor Au concentration and gas flows in the redesigned USP. Upon analyze of the sizes and shapes of the obtained nanoparticles it was proposed that these are the influential parameters for controlling the AuNP formation mechanisms in the given USP system. Increasing the precursor Au concentration reinforces the formation of larger AuNPs via DTP, while decreasing it weakens formation of larger AuNPs. When using low gas flows, the AuNPs are formed by both DTP and GTP mechanisms, indicated by the presence of very small particles and bimodal size distributions (mean sizes of 39.4 ± 20.6 nm

Please cite this article in press as: P. Majerič et al., Formation mechanisms for gold nanoparticles in a redesigned Ultrasonic Spray Pyrolysis, Advanced Powder Technology (2017), http://dx.doi.org/10.1016/j.apt.2016.12.013

and 207.9 ± 38.3 nm for 2.5 g/l Au and mean sizes of 38.9 ± 15.1 nm and 91.3 ± 15.2 nm for 0.5 g/l Au). After increasing the gas flows, formation of secondary droplets and the GTP mechanism becomes prevalent in the system, resulting in synthesis of AuNPs a few 10 nm in size, with a narrower size distribution (mean sizes for medium gas flow: 26.7 ± 13.1 nm, 17.7 ± 6.9 nm, for high gas flow: 45.5 ± 12.5 nm, 37.0 ± 5.5 nm; for both Au concentrations). Favorable control of AuNP formation was achieved with using a low Au concentration (0.5 g/l) with high gas flows (4.5 l/min N2 and 2.0 l/min H2). This has led to relatively more uniform, spherical AuNPs in a narrow size range (37.0 ± 5.5 nm), reaching our desired sizes. In our future work, these formation mechanisms will be examined on other Au precursors with the redesigned USP.

Acknowledgements

The research was carried out under the Young Researcher Program funded by the Slovenian Research Agency (ARRS) and the Project L2-4212: "Gold nanoparticle production technology".

References

[1] A. Lähde, I. Koshevoy, T. Karhunen, T. Torvela, T.A. Pakkanen, J. Jokiniemi, Aerosol-assisted synthesis of gold nanoparticles, J. Nanopart. Res. 16 (2014) 1–8, http://dx.doi.org/10.1007/s11051-014-2716-4.

[2] J.H. Bang, K.S. Suslick, Applications of ultrasound to the synthesis of nanostructured materials, Adv. Mater. 22 (2010) 1039–1059, http://dx.doi.org/10.1002/adma.200904093.

[3] M. Eslamian, M. Ahmed, N. Ashgriz, Modeling of solution droplet evaporation and particle evolution in droplet-to-particle spray methods, Dry. Technol. 27 (2009) 3–13, http://dx.doi.org/10.1080/07373930802565665.

[4] O.B. Milosevic, L. Mancic, M.E. Rabanal, L.S. Gomez, K. Marinkovic, Aerosol route in processing of nanostructured functional materials, KONA Powder Part. J. 27 (2009) 84–106, http://dx.doi.org/10.14356/kona.2009010.

[5] T.T. Kodas, M.J. Hampden-Smith, Aerosol Processing of Materials, first ed., Wiley-VCH, New York, 1998.

[6] K. Otto, I. Oja Acik, M. Krunks, K. Tõnsuaadu, A. Mere, Thermal decomposition study of $HAuCl_4{\cdot}3H_2O$ and $AgNO_3$ as precursors for plasmonic metal nanoparticles, J. Therm. Anal. Calorim. 118 (2014) 1065–1072, http://dx.doi.org/10.1007/s10973-014-3814-3.

[7] Y. Shang, C. Min, J. Hu, T. Wang, H. Liu, Y. Hu, Synthesis of gold nanoparticles by reduction of $HAuCl_4$ under UV irradiation, Solid State Sci. 15 (2013) 17–23, http://dx.doi.org/10.1016/j.solidstatesciences.2012.09.002.

[8] Future Markets, The Global Market for Gold Nanoparticles, 2010–2025, Future Mark. Inc., 2015. <http://www.futuremarketsinc.com/global-market-gold-nanoparticles-2010-2025/> (accessed January 20, 2016).

[9] P. Tiwari, K. Vig, V. Dennis, S. Singh, Functionalized gold nanoparticles and their biomedical applications, Nanomaterials 1 (2011) 31–63, http://dx.doi.org/10.3390/nano1010031.

[10] A.K. Khan, R. Rashid, G. Murtaza, A. Zahra, Gold nanoparticles: synthesis and applications in drug delivery, Trop. J. Pharm. Res. 13 (2014) 1169–1177, http://dx.doi.org/10.4314/tjpr.v13i7.23.

[11] S. Mohammadnejad, J.L. Provis, J.S.J. van Deventer, Reduction of gold(III) chloride to gold(0) on silicate surfaces, J. Colloid Interface Sci. 389 (2013) 252–259, http://dx.doi.org/10.1016/j.jcis.2012.08.053.

[12] A.S. Barnard, Y. Chen, Kinetic modelling of the shape-dependent evolution of faceted gold nanoparticles, J. Mater. Chem. 21 (2011) 12239, http://dx.doi.org/10.1039/c1jm11677k.

[13] M. Rai, N. Duran (Eds.), Metal Nanoparticles in Microbiology, Springer Berlin Heidelberg, Berlin, Heidelberg, 2011. <http://link.springer.com/10.1007/978-3-642-18312-6> (accessed January 11, 2016).

[14] J. Vicente, J. Pinto, J. Menezes, F. Gaspar, Fundamental analysis of particle formation in spray drying, Powder Technol. 247 (2013) 1–7, http://dx.doi.org/10.1016/j.powtec.2013.06.038.

[15] S.C. Tsai, Y.L. Song, C.S. Tsai, C.C. Yang, W.Y. Chiu, H.M. Lin, Ultrasonic spray pyrolysis for nanoparticles synthesis, J. Mater. Sci. 39 (2004) 3647–3657, http://dx.doi.org/10.1023/B:JMSC.0000030718.76690.11.

[16] G.V. Jayanthi, S.C. Zhang, G.L. Messing, Modeling of solid particle formation during solution aerosol thermolysis: the evaporation stage, Aerosol Sci. Technol. 19 (1993) 478–490, http://dx.doi.org/10.1080/02786829308959653.

[17] A.A. Bandyopadhyay, A.A. Pawar, C. Venkataraman, A. Mehra, Modelling size and structure of nanoparticles formed from drying of submicron solution aerosols, J. Nanopart. Res. 17 (2015), http://dx.doi.org/10.1007/s11051-014-2842-z.

[18] P. Majerič, B. Friedrich, R. Rudolf, Au-nanoparticle synthesis via ultrasonic spray pyrolysis with a separate evaporation zone, Mater. Tehnol. 49 (2015) 791–796, http://dx.doi.org/10.17222/mit.2014.264.

[19] P. Majerič, D. Jenko, B. Budič, S. Tomić, M. Čolić, B. Friedrich, R. Rudolf, Formation of non-toxic Au nanoparticles with bimodal size distribution by a modular redesign of ultrasonic spray pyrolysis, Nanosci. Nanotechnol. Lett. 7 (2015) 920–929, http://dx.doi.org/10.1166/nnl.2015.2046.

[20] J. Bogović, A. Schwinger, S. Stopic, J. Schröder, V. Gaukel, H.P. Schuchmann, B. Friedrich, Controlled droplet size distribution in ultrasonic spray pyrolysis, Metall 65 (2011) 455–459.

[21] M. Wuithschick, A. Birnbaum, S. Witte, M. Sztucki, U. Vainio, N. Pinna, K. Rademann, F. Emmerling, R. Kraehnert, J. Polte, Turkevich in new robes: key questions answered for the most common gold nanoparticle synthesis, ACS Nano 9 (2015) 7052–7071, http://dx.doi.org/10.1021/acsnano.5b01579.

[22] P. Pedrosa, R. Vinhas, A. Fernandes, P. Baptista, Gold nanotheranostics: proof-of-concept or clinical tool?, Nanomaterials 5 (2015) 1853–1879, http://dxdoi.org/10.3390/nano5041853.

[23] C.A. Schneider, W.S. Rasband, K.W. Eliceiri, NIH Image to ImageJ: 25 years of image analysis, Nat. Methods 9 (2012) 671–675, http://dx.doi.org/10.1038/nmeth.2089.

[24] G.H. Woehrle, J.E. Hutchinson, S. Özkar, R.G. Finke, Analysis of nanoparticle transmission electron microscopy data using a public-domain image-processing program, image, Turk. J. Chem. 30 (2006) 1–13.

[25] E.S. Clark, D.H. Templeton, C.H. MacGillavry, The crystal structure of gold(III) chloride, Acta Crystallogr. 11 (1958) 284–288, http://dx.doi.org/10.1107/S0365110X58000694.

[26] R.G. Palgrave, I.P. Parkin, Aerosol assisted chemical vapor deposition of gold and nanocomposite thin films from hydrogen tetrachloroaurate(III), Chem. Mater. 19 (2007) 4639–4647, http://dx.doi.org/10.1021/cm0629006.

[27] S. Stopic, R. Rudolf, J. Bogovic, P. Majerič, M. Čolić, S. Tomić, Synthesis of Au nanoparticles prepared by ultrasonic spray pyrolysis and hydrogen reduction, Mater. Tehnol. 47 (2013) 577–583.

Please cite this article in press as: P. Majerič et al., Formation mechanisms for gold nanoparticles in a redesigned Ultrasonic Spray Pyrolysis, Advanced Powder Technology (2017), http://dx.doi.org/10.1016/j.apt.2016.12.013